Stabilizing Role of Itinerant Ferromagnetism in Intergranular Cohesion in Iron

D. Yeşilleten,[1] M. Nastar,[2] T. A. Arias,[1] A. T. Paxton,[2] and S. Yip[2]
[1]*Department of Physics, Massachusetts Institute of Technology, Cambridge, Massachusetts 02139*
[2]*Department of Nuclear Engineering, Massachusetts Institute of Technology, Cambridge, Massachusetts 02139*

(Received 23 September 1997; revised manuscript received 16 March 1998)

We present a simple, general energy functional for ferromagnetic materials based upon a local spin density extension to the Stoner theory of itinerant ferromagnetism. The functional reproduces well available *ab initio* results and experimental interfacial energies for grain boundaries in iron. The model shows that intergranular cohesion along symmetric tilt boundaries in iron depends strongly upon the magnetic structure at these interfaces and illuminates the underlying mechanisms. [S0031-9007(98)07289-5]

PACS numbers: 75.50.Bb

Iron and its steel alloys exhibit two distinct outstanding physical properties, high strength and high magnetic response. Little is known about the direct relationship, if any, between the microscopic origins of these properties. The exchange interaction, preference for alignment of spins to reduce interelectronic Coulomb repulsion through the statistical avoidance of fermions, drives itinerant ferromagnetism. Fundamental topological excitations of the crystalline lattice govern mechanical response: dislocations mediate plasticity; grain boundaries control microstructure and intergranular cohesion. In this Letter we present a new model for itinerant ferromagnetic iron and demonstrate that the exchange interaction plays a significant stabilizing role in grain boundaries, thereby contributing to the strength of intergranular cohesion.

The fundamental role played by exchange in controlling the mechanical response of magnetic materials is at present poorly understood for lack of an appropriate microscopic theory. Studies in iron to date are limited to either full-blown *ab initio* spin-dependent electronic structure calculations [1] or simple interatomic potentials such as the embedded atom method (EAM) [2]. While describing the relevant physics, *ab initio* calculations treat explicitly *too many* degrees of freedom to allow studies of the complex structures of all but the simplest extended defects. For this reason, total energy *ab initio* studies of iron to date have been limited to small clusters exploring the behavior of the simplest [$\Sigma = 3(111)$] grain boundary [3–5]. Interatomic potentials, while practical for complex systems, deal with *too few* degrees of freedom to treat itinerant exchange properly. Nonetheless, these potentials have been useful in studies of grain boundaries [6], dislocations [7], and even fracture [8]. Energies calculated for grain boundaries with the EAM [6], however, are exaggerated by about a factor of 2 when compared with experimental values [9], beginning to approach even the experimental surface energy [10]. Here, we present a simple, general model which gives much better results and reveals the mechanisms stabilizing the boundaries.

In response to the above weakness, Krasko [11] has introduced recently an atomistic potential which includes a prescription for estimating the exchange energy of each atom from its local environment. Here, we follow an alternate, microscopic route. In accord with the microscopic origin of itinerant ferromagnetism, we consider the extended nature of the electrons and determine only the spin-moment coupling constant, the Stoner parameter [12], as a function of the local atomic environment.

Microscopic approach.—Such intermediate, electronic structure based descriptions of iron have been developed in previous studies of iron [13,14], but for ideal crystalline systems. Our approach to the study of defects is to first identify the smallest, physically reasonable set of degrees of freedom from these studies and then extend this treatment to include inhomogeneous systems.

Hasegawa and Pettifor [13] reproduce the experimental $P - T$ phase diagram of iron by combining a tight-binding description of the d bands with a treatment of spin-fluctuation effects. They note that as $T \rightarrow 0$, spin-fluctuation effects become unimportant and their spin-fluctuation theory reduces to the traditional mean-field Stoner theory of itinerant ferromagnetism [12] at a temperature $T_f \approx 500$ K. Zhong, Overney, and Tomanek [14] take up the fact that mean-field Stoner theory is sufficient at room temperature and build a model for bulk crystalline iron based upon an spd tight-binding Hamiltonian and Stoner theory, treating only the mean atomic spins.

We therefore identify a minimal set of active physical degrees of freedom below T_f to consist of the net mean spin moment on each atom and single particle states constructed from atomiclike d orbitals. To pass beyond perfect crystalline material, we introduce a local atomic spin-density extension to Stoner theory.

Construction of energy functional.—Our selected degrees of freedom are (i) the linear combination coefficients $\psi_{nk}(i, m_z)$ describing the bonding among the $m_z = -2, \dots, 2$ atomic d states of each atom i for each band n and each point in the Brillioun zone k, (ii) the net spin $n_\sigma(i)$, $\sigma = \pm 1$, associated with each atom i, and (iii) the location $\vec{\tau}_i$ of each atom i.

To describe the bonding contribution to the energy ϵ_{nk} associated with each single-particle orbital, we use an orthogonal two-center tight-binding Hamiltonian description [15]. In the usual fashion, we take the diagonal elements of the matrix of hopping integrals among L_z eigenstates for two atoms separated by a distance τ along the z axis, $dd\delta, dd\pi, dd\sigma, dd\pi, dd\delta$, to decay exponentially with distance, $dd\lambda = dd\lambda_o e^{-q\tau}$. To set the primitive matrix elements $dd\lambda_o$ and the decay factor q we insist that the tight-binding Hamiltonian reproduces well the *ab initio* density of states for the d bands, which is accomplished by setting the Slater-Koster parameters to $dd\sigma_o = -1$ Ry, $dd\pi_o = 1$ Ry, $dd\delta_o = -0.5$ Ry, and the decay factor to $q = 0.638\,72$ bohr^{-1}.

In summing over the single particle energies, we replace the integral over the Brillouin zone with a discrete sum with appropriate weights w_k [16]. The tendency of our system to spin polarize requires us to consider separate Fermi occupation numbers $f_{nk\sigma}$ for each spin channel σ. We also include the fermionic entropy

$$s_{nk\sigma} \equiv -k_B[f_{nk\sigma} \ln f_{nk\sigma} + (1 - f_{nk\sigma}) \ln(1 - f_{nk\sigma})],$$

so that our band structure energy appears as the first sum in the energy functional (1), where the ϵ_{nk} are the eigenvalues of the tight-binding Hamiltonian. All of the results below are computed at $T = 300$ K.

Combining the Fermi occupations $f_{nk\sigma}$ with the expansion coefficients $\psi_{nk\sigma}$ yields the local atomic spin densities, $n_\sigma(i) \equiv \sum_{n,k,m} w_k f_{nk\sigma} |\psi_{nk}(i,m)|^2$. The Stoner theory of itinerant ferromagnetism describes an energetic *benefit* of polarization due to exchange of magnitude $N_{\mathrm{at}} I m^2/4$, where N_{at} is the total number of atoms in the crystal, m is the spin polarization per atom, and I is the Stoner parameter [12]. To extend this theory beyond homogeneous bulk systems, we introduce a local approximation to the exchange energy in the same spirit as the local-density approximation [17] of density functional theory [18]. In particular, for an inhomogeneous system, we associate a separate energy contribution to the exchange from each atom equal to what we would expect on a per atom basis from a homogeneous system consisting of atoms in the identical environment with identical spin polarization. This contribution appears as the second sum in our energy functional (1). The physical motivation for this approximation is that the itinerant nature of magnetism in iron tends to smooth variations in the spin polarization, limiting the effects of gradient corrections. This approach has the advantage of allowing us to draw upon *ab initio* values of the Stoner exchange parameter in bulk.

Krasko [19] has performed *ab initio* linear response theory calculations of the Stoner parameter I in bcc and fcc bulk iron and found it to have a mild, approximately linear volume dependence, $dI/ds = -0.01$ Ry/bohr, where s is the Wigner-Seitz (WS) radius, and to have slightly different values for the bcc and fcc lattices, $I^o_{\mathrm{bcc}} = 0.072$ Ry$/\mu_B^2$ and $I^o_{\mathrm{fcc}} = 0.069$ Ry$/\mu_B^2$ at $s = 2.66$ bohr. The use of these values in our model gives the correct magnetic and nonmagnetic states for the bcc and fcc structures, respectively. However, to yield the correct total energy ordering of states, we have found necessary a slight enhancement of the bulk Stoner parameters to $I^o_{\mathrm{bcc}} = 0.077$ Ry$/\mu_B^2$ and $I^o_{\mathrm{fcc}} = 0.070$ Ry$/\mu_B^2$, which leads to no magnetization in the fcc phase and a bcc phase magnetic moment of 2.56 μ_B/atom, somewhat enhanced relative to the accepted moment.

Going beyond bulk to inhomogeneous systems with intermediate coordinations Q, we make a linear interpolation for I_i between what would be expected at the same WS radius for the bcc ($Q = 8$) and the fcc ($Q = 12$) lattices. We determine the local coordination number Q_i and WS radius s_i for each atom i with the formulation developed by Sawada [20] and the conversion $s_i = R_i(a + b/Q_i + c/Q_i^2)/2$ from his parameter R_i. We find that setting Sawada's coefficients to $\lambda_1 \equiv 4.5023$ bohr^{-1}, $\lambda_2 \equiv 10.6376$ bohr^{-2} and using $a \equiv 1.7144$, $b \equiv -9.0948$, $c \equiv 56.372$ reproduces to within 0.01% the correct coordination numbers and to within 0.3% the correct WS radii for the diamond structure, bcc and fcc lattices when packed at the atomic density of bcc iron. With the Stoner parameters thus determined, we set the filling N_d of the manifold of d states, so that the Fermi level for spin-down electrons in the bcc structure falls precisely at the minimum of the pseudogap in the tight-binding density of states, reproducing the physical behavior observed in *ab initio* calculations. The resulting filling, $N_d = 6.7$ electrons/atom, is in good agreement with the value of $N_d = 7.0$ used successfully in [13].

Finally, for the energy associated with the locations of the atoms, we take a power-law relationship between the interatomic potential and the hopping elements, a standard successful practice in tight-binding calculations [21], to produce the final term in (1). We fit the two parameters b and p to the experimental equilibrium lattice constant and bulk modulus for the bcc phase of iron, yielding $p = 2.2355$ bohr^{-1} and $b = 872.5174$ Ry, respectively. The ratio $\lambda \equiv p/q$ corresponds to a *normalized hardness* [21], $\alpha_h \equiv (\lambda - 1)/\lambda \approx 0.7$, in line with the values near two-thirds observed previously in tight-binding descriptions of the transition metals [22].

Our final energy functional is thus

$$\begin{aligned} E(\{\vec{\tau}_i\}) = \min_{\psi,f}{}' \Bigg\{ & \sum_{nk\sigma} w_k (f_{nk\sigma}\epsilon_{nk} - T s_{nk\sigma}) \\ & - \frac{1}{4} \sum_i I_i [n_\uparrow(i) - n_\downarrow(i)]^2 \\ & + \frac{b}{2} \sum_{i \neq j} e^{-p\tau_{ij}} \Bigg\}, \end{aligned} \qquad (1)$$

The constraints on the minimization are Fermi statistics, $0 \leq f_{nk\sigma} \leq 1$, and the total number of d electrons, $N_d = \sum_{nk\sigma} w_k f_{nk\sigma}$. This formulation is equivalent *in bulk systems* to the familiar formulation of the Stoner theory in terms of a rigid shift between the up and down electronic density of states, but has the advantage in treating complex structures of allowing distinct local

Stoner parameters to be applied to each atom according to its environment.

Verification.—In bulk, we reproduce the correct energy ordering of phases (bcc-hcp-fcc), finding $E_{\mathrm{hcp}} - E_{\mathrm{bcc}} = 2.2$ mRy/atom and $E_{\mathrm{fcc}} - E_{\mathrm{bcc}} = 6.5$ mRy/atom. Our fcc-bcc energy difference is on the order of what is found in other calculations [13] and theoretical and experimental extrapolation [23,24]. In agreement with *ab initio* calculations [25,26], we observe that the hcp phase is more stable than the nonmagnetic fcc phase for all values of the WS radius. We predict a pressure-induced phase transition from the bcc to the hcp phase at a WS radius of $s = 2.6$ bohr, in good agreement with the *ab initio* studies of [24,27]. (Note that we did not fit our parameters to produce the two preceeding properties.) The small energy differences among these phases open the question of mechanical stability. Our Hamiltonian gives a mechanically stable ferromagnetic bcc phase, even along the Bain transformation ($C' > 0$). Our predicted C' and C_{44}, which we have made no attempt to fit, are about 25% lower than observed experimentally, corresponding to an underestimation of about 12% in the frequencies in the long-wavelength portion of the phonon spectrum.

The experimental literature determines an average typical grain boundary energy in α iron, and the *ab initio* literature provides the spin moment distribution of the $\Sigma = 5(310)$ and $\Sigma = 3(111)$ boundaries and the atomic relaxation of the $\Sigma = 3(111)$ boundary. Table I summarizes our results for these and two other symmetric tilt boundaries. Our calculations were carried out in supercells containing two oppositely oriented boundaries separated by at least 16 layers of atoms. We performed full structural and supercell relaxations of these boundaries.

Table I shows that our energy results are in good agreement with the experimental studies, which set the mean typical grain boundary energy to be approximately 770 erg/cm^2 [9]. [The $\Sigma = 3(112)$ boundary, the coherent twin, is a known special case expected to be unrepresentatively low in energy.] The structural and magnetic predictions of our energy functional are in excellent quantitative agreement with the *ab initio* predictions for the outward structural relaxation of the atomic planes of the $\Sigma = 3(111)$ boundary and for the fractional enhancement of the spin moments on the symmetry plane for both the $\Sigma = 5(310)$ and $\Sigma = 3(111)$ boundaries. (See Δz and Δm in Table I.)

Finally, Fig. 1 shows the detailed spatial distribution of spin moments in the vicinity of the $\Sigma = 5(310)$ boundary. The figure shows that our model not only reproduces the enhancement of moments on the symmetry plane but also predicts correctly the tendency for the spin to fall below the bulk moment before eventually heading back to the bulk value as one moves away from the boundary. Although the figure shows some discrepancies among the details of the two sets of predictions, the agreement which we find supports the fundamental soundness of our approach and its ability to capture the basic physics of and make accurate predictions for complex structures in iron.

Exchange stabilization of grain boundaries in iron.—The fact that the embedded atom model consistently exaggerates boundary energies in iron by a factor of 2 over our functional points to the participation in boundary energetics of a microscopic mechanism more subtle than simple distortions of the metallic bonding network. The data in Table I show that the exchange interaction is a major factor in the physics of the grain boundaries. The tendency to minimize the exchange contribution drives the system to lower its energy at the expense of an almost, but not quite, compensating dramatic increase in the atomic and band structure contributions. The end result of this balance is the lower and much more realistic set of boundary energies in Table I.

Breakdown of the large negative contributions from the exchange interaction shows that the enhancement

TABLE I. Summary of grain-boundary results: Boundary formation energy (E_{gb}), exchange contribution to the energy (E_{ex}), change in magnetic moment on the boundary plane (Δm), maximum Stoner parameter ($\Delta I_{\max}$), and outward motion of planes immediately neighboring the boundary (Δz). Results of other studies appear in parentheses.

Boundary	E_{gb} (erg/cm^2)	E_{ex} (erg/cm^2)	Δm (%)	$\Delta I_{\max}$ (%)	Δz (bohr)
$\Sigma = 3(112)$	140 (300$^{\mathrm{b}}$)	-8600	14	2	0.1
$\Sigma = 5(310)$	560 (1300$^{\mathrm{b}}$) ($\sim$770$^{\mathrm{a}}$)	-3800	9 (8$^{\mathrm{c}}$)	3	0.5
$\Sigma = 3(111)$	770	-5200	18 (15$^{\mathrm{d}}$–18$^{\mathrm{e}}$)	4	0.6 (0.5–0.8$^{\mathrm{e}}$)
$\Sigma = 9(114)$	760 (1450$^{\mathrm{b}}$) ($\sim$770$^{\mathrm{a}}$)	-4100	15	4	0.9

Expt: [a][9]. EAM: [b][6]. *Ab initio*: [c][28]; [d][3]; [e][5].

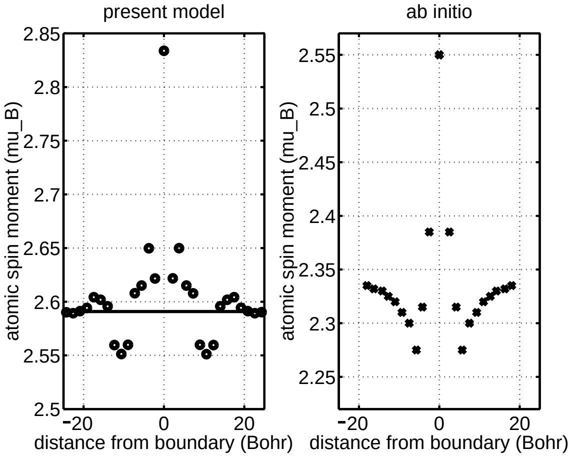

FIG. 1. Prediction of atomic spin moments in the vicinity of the $\Sigma = 5(310)$ symmetric tilt boundary in iron. Left: Present model; Right: *ab initio* results of [28]. Horizontal line gives the bulk phase moment of our calculation.

comes mostly from an increase by 10%–20% of the atomic spin moments with a lesser contribution from an increase by 2%–4% of the Stoner exchange parameters themselves (Table I.) The increase in magnetic moments along the boundary therefore plays a key role in stabilizing the boundaries.

The origin of the increase in moments is the fact that the states in the energy range which contributes to the spin moments in the system tend to be more localized on the grain boundary. States with energy below both Fermi levels $\mu_\uparrow$ and $\mu_\downarrow$ are filled equally with up and down spins and so contribute nothing to the net moment, as do the completely empty states with energies above both Fermi levels. Only those states with energies between the Fermi levels are filled with uncompensated spins and can contribute to the net spin moments. The states in this energy range tend to localize on the boundary as a direct consequence of the more open structure of the boundary, which lowers the tight-binding matrix elements $dd\lambda$ and thereby narrows the band toward the band center. We have confirmed this latter behavior by direct inspection of the electronic states.

Our model also sheds light on the mechanisms underlying structural relaxation of the grain boundaries. In all boundaries in our study, the two planes of atoms immediately neighboring the symmetry plane relax outward and compress into the surrounding bulk. This relaxation pattern is also observed in the *ab initio* calculations of the $\Sigma = 3(111)$ boundary [5]. Because the Stoner parameter increases with compression of the lattice [19], the exchange interaction provides a driving force for this relaxation pattern. In particular, the compression of the planes neighboring the symmetry plane into the surrounding bulk increases the Stoner parameters for a total of four layers of atoms, the two moving layers and the two bulk layers into which they are compressed on either side of the boundary.

In conclusion, we have developed a local spin density functional description of itinerant ferromagnetic materials which provides a simple and accurate picture of the relationships among geometry, magnetization, relaxation, and stability for tilt grain boundaries in iron.

This work was supported by the MRSEC Program of the National Science Foundation (DMR 94-00334) and by the Alfred P. Sloan Foundation (BR-3456). Computational support was provided by the MIT Xolas prototype SUN cluster.

[1] M. C. Payne *et al.*, Rev. Mod. Phys. **64**, 1045 (1992).
[2] M. W. Finnis and J. E. Sinclair, Philos. Mag. A **50**, 45 (1984); **53**, 161 (1984).
[3] G. L. Krasko, in *Defect-Interface Interactions Symposium, Boston, MA*, edited by E. P. Kvam, A. H. King, M. J. Mills, T. D. Sands, and V. Vitek, MRS Symposia Proceedings Vol. 319 (Materials Research Society, Pittsburgh, 1994), p. 369.
[4] Y. Itsumi and D. E. Ellis, J. Mater. Res. **11**, 2214 (1996).
[5] Ruqian Wu, A. J. Freeman, and G. B. Olson, Phys. Rev. B **53**, 7504 (1996).
[6] R. Watanabe, A. Nogami, and T. Matsumiya, Mater. Sci. Forum **204–206**, 337 (1996).
[7] D. Farkas and P. L. Rodriguez, Scr. Metall. **30**, 921 (1994).
[8] K. S. Cheung and S. Yip, Model. Simul. Mater. Sci. Eng. **2**, 865 (1994).
[9] L. H. Van Vlack, Trans. Am. Inst. Min. Metall. Eng. **191**, 251 (1951).
[10] W. Missol, Acta Metall. **24**, 73 (1976).
[11] Genrich L. Krasko, J. Appl. Phys. **79**, 4682 (1996).
[12] E. C. Stoner, Proc. R. Soc. London A **169**, 339 (1939).
[13] H. Hasegawa and D. G. Pettifor, Phys. Rev. Lett. **50**, 130 (1983).
[14] W. Zhong, G. Overney, and D. Tomanek, Phys. Rev. B **47**, 95 (1993).
[15] J. C. Slater and G. F. Koster, Phys. Rev. **94**, 1498 (1954).
[16] H. J. Monkhorst and J. D. Pack, Phys. Rev. B **13**, 5188 (1976).
[17] W. Kohn and L. J. Sham, Phys. Rev. **140**, A1133 (1965).
[18] P. Hohenberg and W. Kohn, Phys. Rev. **136**, B864 (1964).
[19] G. L. Krasko, Solid State Commun. **70**, 1099 (1989).
[20] S. Sawada, Vacuum **41**, 612 (1990).
[21] D. Pettifor, *Bonding and Structure of Molecules and Solids* (Clarendon Press, Oxford, 1995), pp. 78–79.
[22] *Bonding and Structure of Molecules and Solids* (Ref. [21]), p. 188.
[23] L. Kaufman and H. Bernstein, *Computer Calculations of Phase Diagrams* (Academic Press, New York, 1970).
[24] W. Bendick and W. Pepperhof, Acta Metall. **30**, 679 (1982).
[25] A. T. Paxton, M. Methfessel, and H. M. Polatoglou, Phys. Rev. B **41**, 8127 (1990).
[26] L. Stixrude, R. E. Cohen, and D. J. Singh, Phys. Rev. B **50**, 6442 (1994).
[27] P. Soderlind, R. Ahuja, O. Eriksson, J. M. Wills, and B. Johansson, Phys. Rev. B **50**, 5918 (1994).
[28] K. Hampel, D. D. Vvedensky, and S. Crampin, Phys. Rev. B **47**, 4810 (1993).